Mineralogical Magazine (2023), **87**, 171–177
doi:10.1180/mgm.2022.123

CAMBRIDGE UNIVERSITY PRESS

Article

Pohlite, a new lead iodate hydroxide chloride from Sierra Gorda, Chile

Anthony R. Kampf[1]*, George E. Harlow[2] and Chi Ma[3]

[1]Mineral Sciences Department, Natural History Museum of Los Angeles County, 900 Exposition Boulevard, Los Angeles, CA 90007, USA; [2]Department of Earth and Planetary Sciences, American Museum of Natural History, 200 Central Park West, New York, NY 10024, USA; and [3]Division of Geological and Planetary Sciences, California Institute of Technology, Pasadena, California 91125, USA

Abstract

The new mineral pohlite (IMA2022–043), $Pb_7(IO_3)(OH)_4Cl_9$, was found at La Compania mine, Sierra Gorda, Antofagasta Province, Antofagasta, Chile, where it occurs in cavities in an oxidised portion of a quartz vein in association with massive aragonite and anhydrite. Pohlite crystals are transparent, colourless to pale grey blades, up to 4 mm in length. The mineral has a white streak, adamantine lustre and is nonfluorescent. It is brittle with irregular, conchoidal fracture. The Mohs hardness is ~2½ and it has no cleavage. The calculated density is 5.838(2) g cm^{-3}. Optically, the mineral is biaxial (+) with $\alpha < 2.01$(est.), $\beta = 2.02$ (calc.), $\gamma = 2.05$ (calc.); $2V = 60(5)°$; moderate $r > v$ dispersion; orientation: $Y \wedge \mathbf{a} \approx 20°$, $Z \wedge \mathbf{b} \approx 30°$; and is nonpleochroic. The Raman spectrum exhibits bands consistent with IO_3^- and O–H. Electron microprobe analysis provided the empirical formula $Pb_{6.74}I_{1.00}Cl_{9.29}O_{6.71}H_{4.23}$. The five strongest powder X-ray diffraction lines are [d_{obs} Å(I)(hkl)]: 3.818(91)(023, 122, 1$\bar{2}$1), 3.674(85)($\bar{1}\bar{2}$1, $\bar{1}$22, 200, 104), 3.399(47)($\bar{2}$10, 210, $\bar{1}$04), 2.378(100)(302, 041, $\bar{2}$24) and 1.9943(45)(multiple). Pohlite is triclinic, $P\bar{1}$, $a = 7.3366(5)$, $b = 9.5130(9)$, $c = 16.2434(15)$ Å, $\alpha = 81.592(7)$, $\beta = 84.955(7)$, $\gamma = 89.565(6)°$, $V = 1117.13(17)$ Å^3 and $Z = 2$. The structure of pohlite ($R_1 = 0.0328$ for 3394 $I > 2\sigma I$) contains two types of clusters, a $[Pb_4(OH)_3]^{5+}$ cluster formed by short Pb–O bonds and a $[Pb_3(OH)(IO_3)]_2^{8+}$ 'double cluster' formed by short I–O bonds and short- to medium-length Pb–O bonds. Long Pb–Cl and I–Cl bonds link the clusters together in three dimensions.

Keywords: pohlite, new mineral, iodate, lone-pair electrons, Pb–(O,OH) clusters, crystal structure, Raman spectroscopy, Sierra Gorda, Chile

(Received 5 October 2022; accepted 2 November 2022; Accepted Manuscript published online: 16 November 2022; Associate Editor: David Hibbs)

Introduction

Cations with lone-pair (non-bonding) valence-shell electrons are well known to exhibit off-centre or 'lopsided' coordinations due to lone-pair – bond-pair interaction, often referred to as the lone-pair effect. In such coordinations, bonds on the side of the cation opposite its lone-pair electrons are significantly shorter than those on the same side as the lone pair. Shorter bonds are generally stronger bonds, so that some cations with lone pairs, such as As^{3+} ($4s^2$ lone pair) and I^{5+} ($5s^2$ lone pair), commonly form strongly bonded anionic groups with O^{2-}, such as the AsO_3^{3-} (arsenite) and IO_3^- (iodate) trigonal pyramidal anions in which three O^{2-} ligands define the base of the pyramid with the cation at its apex. Pb^{2+}, with its $6s^2$ lone pair, exhibits more varied coordinations, commonly with three or four short bonds in the 2.2 to 2.4 Å range, but sometimes with essentially symmetrical coordination spheres in which the lone pair is not stereoactive. The new mineral pohlite, described herein, has a structure that includes two different kinds of cations with lone-pair electrons, Pb^{2+} and I^{5+}. The single I^{5+} in the structure participates in an iodate group, whereas all seven discrete Pb^{2+} cations have stereoactive lone pairs and form short- to medium-length bonds to O atoms, resulting in two different cluster structural units, $[Pb_4(OH)_3]^{5+}$ and $[Pb_3(OH)(IO_3)]_2^{8+}$, both apparently new to science.

Pohlite is named for American economic geologist Demetrius Pohl (b. 1944). Dr. Pohl received his Ph.D. in geochemistry in 1984 from Stanford University, California, USA. In the mid 1980s, he was Assistant Curator of economic geology at the American Museum of Natural History. During that period, he collected at various mines in South America including La Compania mine at Sierra Gorda, Chile, where he discovered the new mineral described herein. After leaving the employ of the American Museum, Dr. Pohl joined a major mining company and then started a company exploring for gold and base-metal deposits principally in South America and Africa. Dr. Pohl has given his permission for the mineral to be named in his honour. The new mineral and name (symbol Poh) were approved by the Commission on New Minerals, Nomenclature and Classification of the International Mineralogical Association (IMA2022-043, Kampf *et al.*, 2022a). The description is based on three cotype specimens. One is deposited in the American Museum of Natural History, New York, New York, USA with catalogue number 115471. Two are deposited in the collections of the Natural History Museum of Los Angeles County, Los Angeles, California, USA with catalogue numbers 76251 and 76252.

***Author for correspondence:** Anthony R. Kampf, Email: akampf@nhm.org
Cite this article: Kampf A.R., Harlow G.E. and Ma C. (2023) Pohlite, a new lead iodate hydroxide chloride from Sierra Gorda, Chile. *Mineralogical Magazine* **87**, 171–177. https://doi.org/10.1180/mgm.2022.123

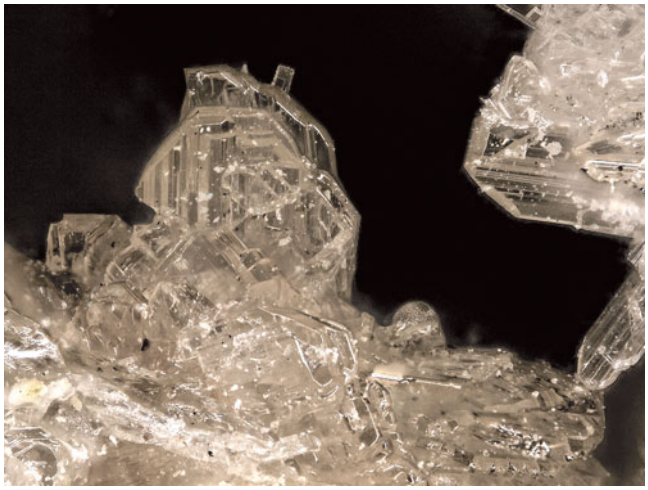

Fig. 1. Pohlite crystals on cotype specimen #76251. The field of view is 1.5 mm across.

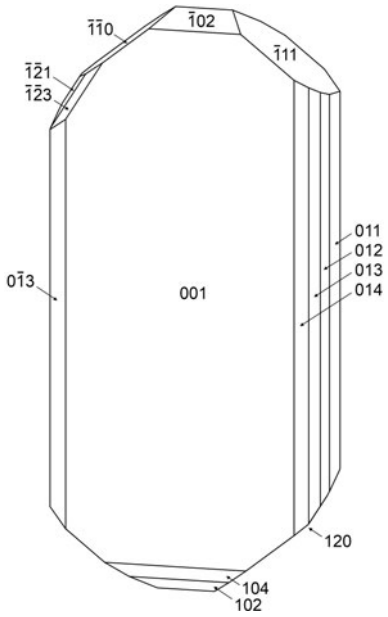

Fig. 2. Crystal drawing of pohlite; clinographic projection with **a** vertical (pointing down).

Occurrence

Pohlite was found by Demetrius Pohl at La Compania mine, Sierra Gorda, Antofagasta Province, Antofagasta, Chile (22° 56′27″S, 69°20′37″W). La Compania mine is located 6 km SW of the town of Sierra Gorda and ~1 km SE of the Pan-American Highway in a range of low hills. La Compania mine exploits a 2–3 m wide, polymetallic, quartz–baryte vein hosted by porphyritic andesites of the lower Cretaceous Quebrada Mala Formation (Williams, 1992). The vein is characterised by banded, crustiform quartz and gangue minerals in a propylitically-altered andesite host rock. Several copper chlorides and supergene native gold comprise the economic mineralisation which extends into fractures several metres beyond the vein margins (Boric *et al.*, 1990). It is surmised that much of the exploited gold mineralisation was precipitated in fractures by evaporation of saline groundwater with a high Br:Cl ratio (0.3), which increased the stability of aqueous Au–Br complexes and permitted solution transport of gold into the wall rocks (Pohl, 1986).

The new mineral occurred in an interior, oxidised portion of the vein in small cavities within massive granular aragonite and anhydrite close to fresh sulfides, ~40 m below the surface and ~50 cm above the water table. In addition to the new mineral, other associated minerals identified in the zone are anhydrite, aragonite, boleite, cotunnite, goethite, gold, hematite, paratacamite, pseudoboleite, saponite and seeligerite.

Physical and optical properties

Pohlite crystals are striated blades, up to ~4 mm in length (Fig. 1). Blades are elongated and striated parallel to [010], flattened on {001} and exhibit the forms {001}, {011}, {012}, {013}, {014}, {$0\bar{1}3$}, {102}, {104}, {$\bar{1}02$}, {$\bar{1}11$}, {110}, {120}, {$12\bar{1}$} and {$123\bar{}$} (Fig. 2). Crystals are colourless to pale grey and transparent with adamantine lustre and a white streak. The mineral is non-fluorescent. The Mohs hardness is ~2½, based on scratch tests. Crystals are brittle with conchoidal fracture and no cleavage. Pohlite becomes cloudy and very slowly dissolves in room-temperature, dilute HCl. The density could not be measured because crystals exceed the density of available density fluids. The calculated density is 5.838 g·cm^{-3} for the empirical formula and 5.975 g·cm^{-3} for the ideal formula.

All indices of refraction for pohlite are >2.00, the highest liquid available to us. Observations of Becke lines in the 2.00 liquid suggest that α is only slightly >2.00. Estimating the value α to be 2.01 allows the calculation of β and γ from the α–β and γ–β birefringences measured with a Berek compensator as 0.010(5) and 0.030(5), respectively. The optical properties are thus: biaxial (+), α = 2.01(est.), β = 2.02 (calc.) and γ = 2.05 (calc.). 2V (meas.) = 60(5)° by direct measurement on a spindle stage and 2V (calc.) = 60.7°. Dispersion is $r > v$ moderate. The partially determined optical orientation is $Y \wedge \mathbf{a} \approx 20°$ and $Z \wedge \mathbf{b} \approx 30°$. No pleochroism was observed. The Gladstone–Dale compatibility index $1 - (K_P/K_C)$ is –0.025 (excellent) for the empirical formula and –0.013 (superior) for the ideal formula (Mandarino, 2007).

Raman spectroscopy

Raman spectroscopy was conducted on a Horiba XploRA PLUS using a 532 nm diode laser, 50 μm slit, 2400 gr/mm diffraction grating and a 100× (0.9 NA) objective. The spectrum for pohlite from 4000 to 60 cm^{-1} is shown in Fig. 3. The bands between 3700 and 3100 cm^{-1} are consistent with the O–H stretching vibrations [labelled ν(O–H) in Fig. 3]. Most other bands in the spectrum are probably attributable to the various stretching and bending modes of the iodate group (see Schellenschläger *et al.*, 2001; Girase *et al.*, 2013). In Fig. 3, these are tentatively labelled as follows: ν_1(I–O) = I–O symmetric stretching, ν_3(I–O) = I–O asymmetric stretching, ν_2(I–O) = I–O symmetric bending and δ_4(I-O) = I–O asymmetric bending. However, it should be noted that some of the bands between 400 and 60 cm^{-1} are probably related to Pb–O stretching and bending modes (see Jensen, 2002; Welch *et al.*, 2016).

Chemical composition

Analyses of pohlite (3 points) were performed at Caltech on a JEOL 8200 electron microprobe in wavelength dispersive spectroscopy mode. Analytical conditions were 15 kV accelerating

https://doi.org/10.1180/mgm.2022.123 Published online by Cambridge University Press

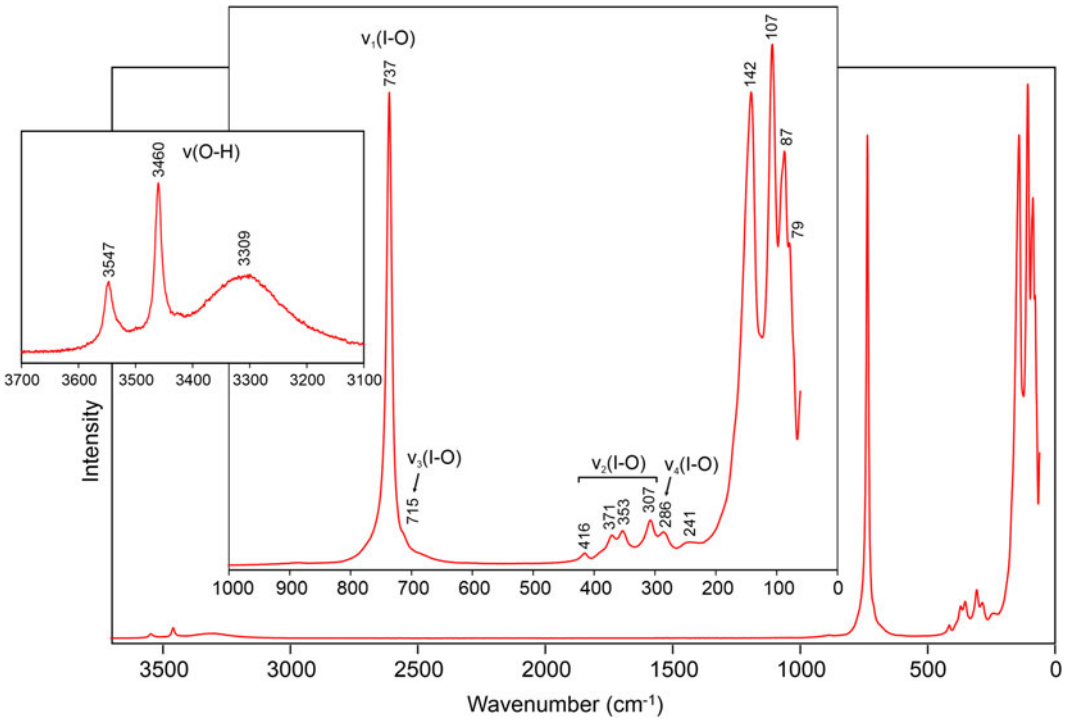

Fig. 3. Raman spectrum of pohlite recorded with a 532 nm laser.

voltage, 10 nA beam current and 5 μm beam diameter. We generally observed higher Cl analyses than were expected on the basis of the structure determination. Insufficient material is available for the determination of H_2O, so it is calculated based on the structure. Analytical data are given in Table 1. The empirical formula (calculated on the basis of O + Cl =16 atoms per formula unit) is $Pb_{6.74}I_{1.00}Cl_{9.29}O_{6.71}H_{4.23}$. The ideal formula is $Pb_7(IO_3)(OH)_4Cl_9$, which requires PbO 77.64, I_2O_5 8.29, Cl 15.86, H_2O 1.79, O = Cl −3.58, total 100 wt.%.

X-ray crystallography and structure refinement

Powder X-ray diffraction was done using a Rigaku R-Axis Rapid II curved imaging plate microdiffractometer, with monochromatised Mo*K*α radiation. A Gandolfi-like motion on the φ and ω axes was used to randomise the sample and observed *d*-values and intensities were derived by profile fitting using *JADE Pro* software (Materials Data, Inc.). The powder data are presented in Supplementary Table S1. Unit cell parameters refined from

Table 1. Chemical composition (in wt.%) for pohlite.

Constituent	Mean	Range	S.D.	Standard
PbO	78.88	78.74–79.02	0.14	PbS
I_2O_5	8.75	8.66–8.88	0.12	RbI
Cl	17.28	16.83–17.62	0.41	sodalite
H_2O*	2.00			
O=Cl	−3.90			
Total	103.01			

*Based on the structure.
S.D. – standard deviation

Table 2. Data collection and structure refinement details for pohlite.

Crystal data	
Structural formula	$Pb_7(IO_3)(OH)_4Cl_9$ (including unlocated H)
Space group	$P\bar{1}$ (#2)
Unit-cell dimensions	a = 7.3366(5) Å
	b = 9.5130(9) Å
	c = 16.2434(15) Å
	α = 81.592(7)°
	β = 84.955(7)°
	γ = 89.565(6)°
V (Å^3)	1117.13(17)
Z	2
Density (for above formula) (g cm^{-3})	5.982
Absorption coefficient (mm^{-1})	55.027
Data collection	
Diffractometer	Rigaku R-Axis Rapid II
X-ray radiation/power	Mo*K*α (λ = 0.71075 Å)/50 kV, 40 mA
Temperature (K)	293(2)
F(000)	1680
Crystal size (μm)	80 × 80 × 80
θ range (°)	3.09 to 25.03
Index ranges	$-8 \le h \le 7$, $-11 \le k \le 11$, $-19 \le l \le 19$
Reflections collected/unique	15819/3941; R_{int} = 0.072
Reflections with $I > 2\sigma I$	3394
Completeness to θ = 30.50°	99.7%
Refinement	
Refinement method	Full-matrix least-squares on F^2
Parameter/restraints	221/0
GoF	1.107
Final R indices [$I > 2\sigma I$]	R_1 = 0.0328, wR_2 = 0.0670
R indices (all data)	R_1 = 0.0414, wR_2 = 0.0709
Largest diff. peak/hole (e^- A^{-3})	+1.70/−1.77

$R_{int} = \Sigma|F_o^2 - F_o^2(\text{mean})|/\Sigma[F_o^2]$. GoF = $S = \{\Sigma[w(F_o^2 - F_c^2)^2]/(n-p)\}^{½}$. $R_1 = \Sigma||F_o| - |F_c||/\Sigma|F_o|$. $wR_2 = \{\Sigma[w(F_o^2 - F_c^2)^2]/\Sigma[w(F_o^2)^2]\}^{½}$; $w = 1/[\sigma^2(F_o^2) + (aP)^2 + bP]$ where a is 0.0163, b is 8.7538 and P is $[2F_c^2 + \text{Max}(F_o^2, 0)]/3$.

https://doi.org/10.1180/mgm.2022.123 Published online by Cambridge University Press

Table 3. Atom coordinates and displacement parameters (Å^2) for pohlite.

	x/a	*y/b*	*z/c*	U_{eq}
Pb1	0.74291(7)	0.42581(6)	0.91662(3)	0.01969(14)
Pb2	0.79848(7)	0.69909(6)	0.70735(3)	0.02094(14)
Pb3	0.74834(7)	0.85567(6)	0.92106(3)	0.02249(15)
Pb4	0.61383(6)	0.20810(6)	0.67053(3)	0.01864(14)
Pb5	0.19352(6)	0.16830(5)	0.82207(3)	0.01608(14)
Pb6	0.23058(7)	0.44608(6)	0.59329(3)	0.01986(14)
Pb7	0.23103(7)	0.01186(6)	0.59162(3)	0.02008(14)
I	0.38916(10)	0.66590(8)	0.85039(4)	0.01114(18)
O1	0.5276(11)	0.5352(9)	0.8022(5)	0.017(2)
O2	0.5285(11)	0.8199(10)	0.8036(5)	0.021(2)
O3	0.4981(11)	0.6392(9)	0.9484(5)	0.0148(19)
OH4	0.8560(11)	0.6642(9)	0.8533(5)	0.0155(19)
OH5	0.3457(11)	0.0515(9)	0.7218(5)	0.0160(19)
OH6	0.3504(11)	0.3377(9)	0.7234(5)	0.0148(19)
OH7	0.3884(11)	0.2329(9)	0.5715(5)	0.0127(19)
H7	0.400(17)	0.265(14)	0.517(8)	0.019
Cl1	0.9059(4)	0.3903(3)	0.74684(18)	0.0185(7)
Cl2	0.1639(4)	0.4151(4)	0.93651(18)	0.0201(7)
Cl3	0.6132(4)	0.5275(4)	0.58762(17)	0.0198(7)
Cl4	0.9589(4)	0.2437(4)	0.5241(2)	0.0270(8)
Cl5	0.6159(4)	0.9301(4)	0.58706(18)	0.0213(7)
Cl6	0.8999(4)	0.9852(4)	0.75465(19)	0.0213(7)
Cl7	0.2034(4)	0.7044(3)	0.69307(18)	0.0197(7)
Cl8	0.1417(5)	0.8610(4)	0.9469(2)	0.0270(8)
Cl9	0.5343(4)	0.1516(4)	0.8882(2)	0.0258(8)

	U^{11}	U^{22}	U^{33}	U^{23}	U^{13}	U^{12}
Pb1	0.0211(3)	0.0207(3)	0.0168(3)	−0.0016(2)	−0.00117(19)	0.0020(2)
Pb2	0.0208(3)	0.0236(3)	0.0182(3)	−0.0028(2)	−0.0009(2)	−0.0002(2)
Pb3	0.0240(3)	0.0231(3)	0.0225(3)	−0.0092(2)	−0.0042(2)	−0.0015(2)
Pb4	0.0146(3)	0.0206(3)	0.0214(3)	−0.0042(2)	−0.00381(19)	0.0001(2)
Pb5	0.0181(3)	0.0187(3)	0.0114(2)	−0.00318(19)	0.00090(18)	−0.0008(2)
Pb6	0.0210(3)	0.0164(3)	0.0216(3)	−0.0010(2)	−0.0015(2)	0.0033(2)
Pb7	0.0218(3)	0.0183(3)	0.0214(3)	−0.0068(2)	−0.0021(2)	−0.0040(2)
I	0.0086(4)	0.0130(5)	0.0119(4)	−0.0017(3)	−0.0011(3)	−0.0002(3)
O1	0.015(5)	0.024(6)	0.014(4)	−0.011(4)	0.003(3)	0.002(4)
O2	0.018(5)	0.020(6)	0.025(5)	−0.003(4)	−0.007(4)	−0.004(4)
O3	0.017(5)	0.018(5)	0.011(4)	−0.004(4)	−0.009(3)	−0.005(4)
OH4	0.009(4)	0.022(5)	0.016(4)	−0.003(4)	0.000(3)	−0.002(4)
OH5	0.023(5)	0.013(5)	0.013(4)	−0.004(4)	−0.002(3)	−0.006(4)
OH6	0.022(5)	0.009(5)	0.013(4)	0.001(3)	0.001(3)	−0.003(4)
OH7	0.018(5)	0.015(5)	0.006(4)	−0.004(4)	0.000(3)	−0.002(4)
Cl1	0.0174(16)	0.0199(19)	0.0189(15)	−0.0058(13)	−0.0001(12)	0.0019(14)
Cl2	0.0208(17)	0.0208(19)	0.0187(16)	−0.0036(13)	−0.0009(12)	0.0001(14)
Cl3	0.0249(17)	0.0211(19)	0.0129(15)	−0.0003(13)	−0.0016(12)	−0.0070(14)
Cl4	0.0153(17)	0.031(2)	0.0352(19)	−0.0060(16)	−0.0028(14)	0.0019(15)
Cl5	0.0275(18)	0.0217(19)	0.0151(15)	−0.0044(13)	−0.0016(13)	0.0083(15)
Cl6	0.0203(17)	0.0178(19)	0.0257(17)	−0.0007(14)	−0.0050(13)	−0.0029(14)
Cl7	0.0206(17)	0.0176(19)	0.0214(16)	−0.0035(13)	−0.0031(13)	−0.0007(14)
Cl8	0.0237(19)	0.027(2)	0.0320(19)	−0.0054(15)	−0.0077(14)	−0.0012(16)
Cl9	0.0249(19)	0.024(2)	0.0320(19)	−0.0092(15)	−0.0119(14)	0.0024(16)

the powder data using *JADE Pro* with whole pattern fitting are: a = 7.336(5), b = 9.526(5), c = 16.245(5) Å, α = 81.582(19), β = 84.904(10), γ = 89.584(14)° and V = 1118.5(8) Å^3.

The single-crystal structure data were collected at room temperature using the same diffractometer and radiation noted above. The Rigaku *CrystalClear* software package was used for processing structure data, including the application of an empirical multi-scan absorption correction using *ABSCOR* (Higashi, 2001). The structure was solved using the intrinsic-phasing algorithm of the *SHELXT* program (Sheldrick, 2015a). *SHELXL-2016* (Sheldrick, 2015b) was used for the refinement of the structure. Difference-Fourier mapping revealed only one likely H site (H7). Data collection and refinement details are given in Table 2, atom coordinates and displacement parameters in Table 3, selected bond lengths in Table 4 and a bond-valence analysis in Table 5. The crystallographic information file has been deposited with the Principal Editor of *Mineralogical Magazine* and is available as Supplementary material (see below).

Description of the structure

There are seven distinct Pb atoms (Pb1 through Pb7) each of which exhibits markedly off-centre coordination typical of Pb^{2+} with stereoactive $6s^2$ lone-pair electrons. There is one I atom with a valence of 5+. Due to its $5s^2$ lone-pair electrons, the I^{5+} also displays off-centre (one-sided) coordination, participating in three short bonds to O atoms (O1, O2 and O3) to yield a trigonal pyramidal IO_3^- iodate anion with I^{5+} at its apex. Short Pb–O

https://doi.org/10.1180/mgm.2022.123 Published online by Cambridge University Press

Table 4. Selected bond lengths (in Å) for pohlite.

Pb1–OH4	2.467(8)	Pb4–OH7	2.393(8)	Pb7–OH7	2.373(8)
Pb1–O1	2.637(8)	Pb4–OH6	2.444(8)	Pb7–OH5	2.424(8)
Pb1–O3	2.693(8)	Pb4–OH5	2.485(8)	Pb7–Cl5	2.921(3)
Pb1–O3	2.775(9)	Pb4–Cl3	3.139(3)	Pb7–Cl5	2.993(3)
Pb1–Cl1	2.973(3)	Pb4–Cl5	3.143(3)	Pb7–Cl4	3.109(4)
Pb1–Cl2	3.132(3)	Pb4–Cl1	3.207(3)	Pb7–Cl7	3.139(3)
Pb1–Cl2	3.133(3)	Pb4–Cl6	3.218(3)	Pb7–Cl6	3.415(3)
Pb1–Cl9	3.146(3)	Pb4–Cl4	3.302(3)	Pb7–Cl4	3.637(4)
Pb1–Cl8	3.406(4)	Pb4–Cl9	3.495(3)	<Pb7–O>	2.399
<Pb1–O>	2.643	<Pb4–O>	2.441	<Pb7–Cl>	3.202
<Pb1–Cl>	3.158	<Pb4–Cl>	3.251		
				I–O1	1.820(8)
Pb2–OH4	2.419(8)	Pb5–OH5	2.307(8)	I–O2	1.825(9)
Pb2–O1	2.750(8)	Pb5–OH6	2.332(8)	I–O3	1.828(7)
Pb2–O2	2.762(9)	Pb5–Cl9	2.801(3)	I–Cl7	2.976(3)
Pb2–Cl7	2.959(3)	Pb5–Cl6	3.147(3)	I–Cl2	3.010(3)
Pb2–Cl1	3.027(3)	Pb5–Cl1	3.168(3)	I–Cl8	3.082(4)
Pb2–Cl6	3.049(3)	Pb5–Cl2	3.195(3)	<I–O>	1.824
Pb2–Cl5	3.098(3)	Pb5–Cl8	3.309(4)	<I–Cl>	3.023
Pb2–Cl3	3.118(3)	<Pb5–O>	2.320		
<Pb2–O>	2.644	<Pb5–Cl>	3.124	Hydrogen bonds	
<Pb2–Cl>	3.050			OH4···Cl7	3.460(8)
		Pb6–OH7	2.384(9)	OH4···Cl8	3.416(9)
Pb3–OH4	2.360(9)	Pb6–OH6	2.444(8)	OH5···O2	2.798(13)
Pb3–O2	2.664(8)	Pb6–Cl3	2.908(3)	OH6···O1	2.811(12)
Pb3–O3	2.731(8)	Pb6–Cl3	3.035(3)	OH7···Cl3	3.187(9)
Pb3–Cl6	2.929(3)	Pb6–Cl7	3.131(3)		
Pb3–Cl8	2.954(3)	Pb6–Cl4	3.167(3)		
Pb3–Cl9	3.212(4)	Pb6–Cl1	3.281(3)		
Pb3–Cl2	3.301(3)	Pb6–Cl4	3.610(4)		
Pb3–Cl9	3.566(3)	<Pb6–O>	2.414		
<Pb3–O>	2.585	<Pb6–Cl>	3.189		
<Pb3–Cl>	3.192				

bonds define two different clusters. The Pb1, Pb2 and Pb3 atoms each form a short bond (2.360 to 2.467 Å) to OH4 yielding a strongly bonded $Pb_3(OH)$ grouping. Each of these Pb atoms also makes two medium-length bonds (2.637 to 2.775 Å) to O atoms in the IO_3^{2-} iodate anion resulting in a $[Pb_3(OH)(IO_3)]$ cluster. The Pb1 atom also forms a medium-length bond (2.693 Å) to the O1 atom in an adjacent $[Pb_3(OH)(IO_3)]$ cluster thereby creating a double Pb1–O1 link and yielding a $[Pb_3(OH)(IO_3)]_2^{8+}$ 'double cluster' (Fig. 4a,b). The second cluster comprises Pb4, Pb5, Pb6, Pb7, OH5, OH6 and OH7. Pb4 forms short bonds

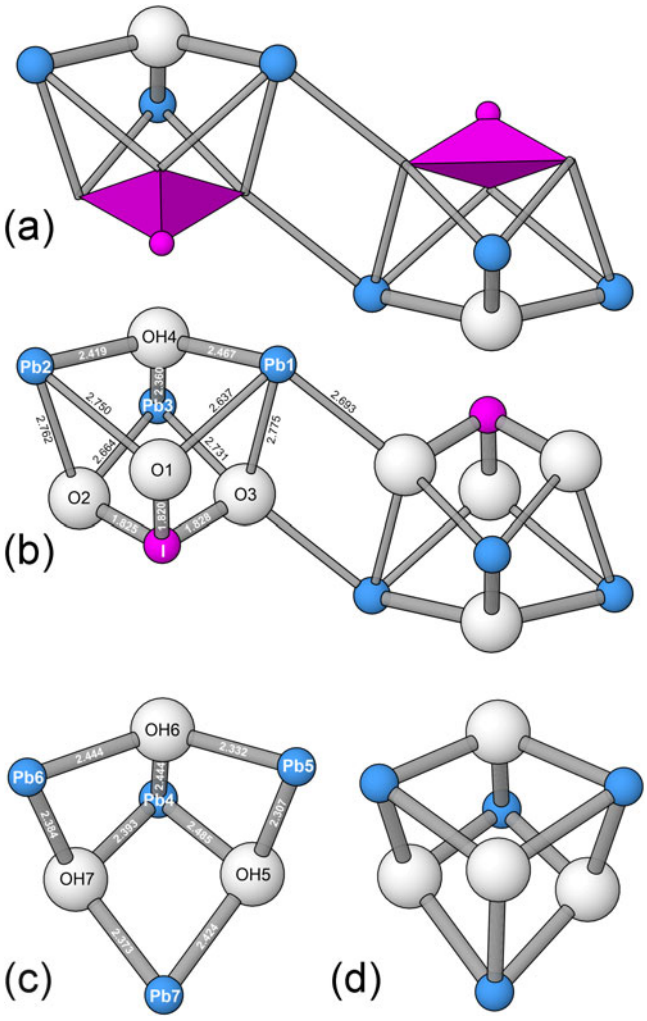

Fig. 4. The $[Pb_3(OH)(IO_3)]_2^{8+}$ 'double cluster' in the structure of pohlite (a) with the iodate group shown as a pyramid and (b) with the iodate group shown in ball-and-stick style. (c) The $[Pb_4(OH)_3]^{5+}$ cluster in the structure of pohlite. (d) The cubane-like $[Pb_4(OH)_4]^{4+}$ cluster in the structure of nitroplumbite. Short Pb–O bonds are shown as thick grey sticks and medium-length Pb–O bonds are shown as thinner grey sticks.

Table 5. Bond-valence sums (in valence units) for pohlite.

	Pb1	Pb2	Pb3	Pb4	Pb5	Pb6	Pb7	I	H	Sum
O1	0.25	0.20						1.44	0.18	2.07
O2		0.19	0.24					1.42	0.18	2.04
O3	0.22, 0.19		0.21					1.41		2.03
OH4	0.37	0.42	0.48						−0.10	1.17
OH5				0.36	0.54		0.41		−0.18	1.12
OH6				0.39	0.51	0.39			−0.18	1.11
OH7				0.44		0.45	0.46		−0.13	1.23
Cl1	0.30	0.26		0.16	0.18	0.13				1.03
Cl2	0.20, 0.20		0.12		0.17			0.18		0.86
Cl3		0.20		0.19		0.36, 0.26			0.13	1.14
Cl4				0.12		0.18, 0.05	0.21, 0.05			0.62
Cl5		0.22		0.19			0.35, 0.29			1.04
Cl6		0.25	0.34	0.16	0.19		0.09			1.02
Cl7		0.31				0.20	0.19	0.20	0.05	0.95
Cl8	0.09		0.32		0.12			0.15	0.05	0.73
Cl9	0.19		0.16, 0.06	0.07	0.48					0.96
Sum	2.02	2.05	1.92	2.09	2.18	2.02	2.05	4.81		

Bond-valence parameters for I^{5+}–Cl^- are from Brese and O'Keeffe (1991). All others are from Gagné and Hawthorne (2015). Hydrogen bond contributions are estimated from $O_D\cdots O_A$ distances using Ferraris and Ivaldi (1988) and from H···Cl distance using Malcherek and Schlüter (2006). We are not aware of a relation for calculating hydrogen bond contributions based on the $O_D\cdots Cl_A$ distance, so we have estimated them as 0.05 valence units for OH4···Cl7 and OH4···Cl8. Negative values indicate donated hydrogen-bond valence.

https://doi.org/10.1180/mgm.2022.123 Published online by Cambridge University Press

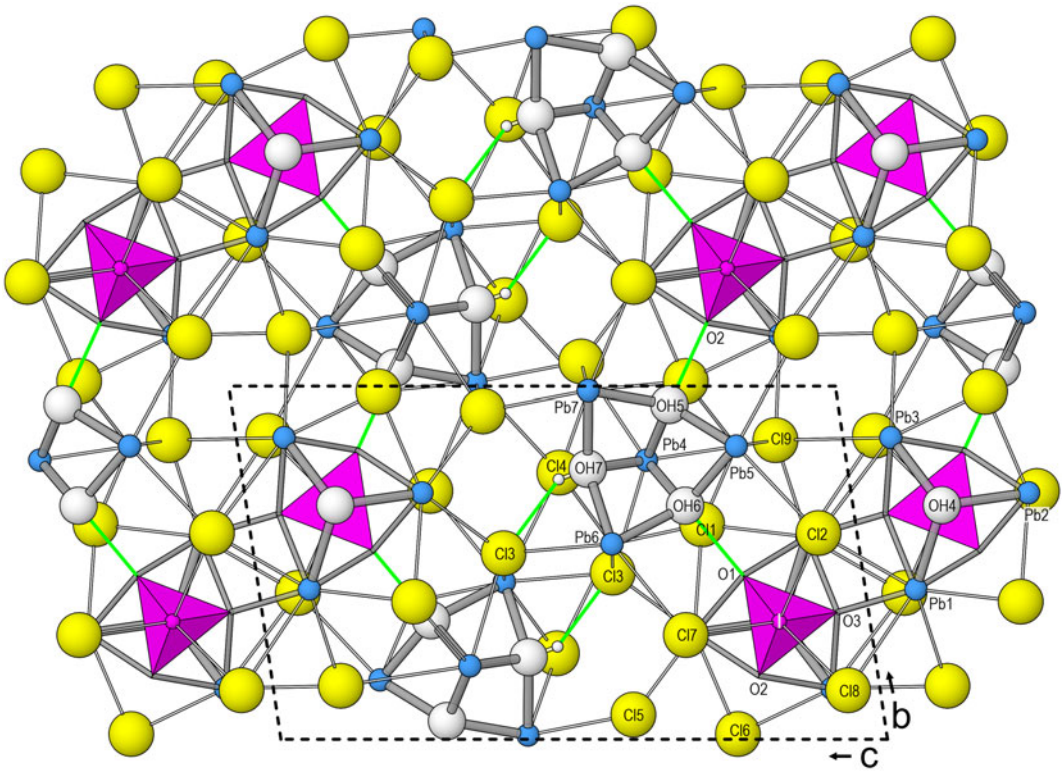

Fig. 5. The structure of pohlite viewed along [100]. Short Pb–O bonds are shown as thick grey sticks, medium-length Pb–O bonds are shown as thinner grey sticks, long Pb–Cl and I–Cl bonds are shown as thin sticks and hydrogen bonds are shown as green lines (OH4···Cl hydrogen bonds are hidden). The unit-cell outline is shown by dashed black lines.

(2.393 to 2.485 Å) to three OH groups and Pb5, Pb6 and Pb7 each form short bonds (2.307 to 2.444 Å) to two OH groups resulting in a $[Pb_4(OH)_3]^{5+}$ cluster (Fig. 4c). There are nine distinct Cl atoms (Cl1 through Cl9). The Pb and I atoms form long bonds to the Cl atoms at Pb–Cl distances from 2.801 to 3.637 Å and I–Cl distances from 2.976 to 3.082 Å. The long bonds Pb–Cl and I–Cl serve to link the clusters together in three dimensions. Additional linkage is provided by hydrogen bonds. The located H7 site indicates a likely hydrogen bond between OH7 and Cl3. Hydrogen bonds from OH5 to O2 and from OH6 to O1 are also clearly indicated. From a geometrical perspective, the only hydrogen bonds likely to be from OH4 are to Cl7 and Cl8. The complete structure is shown in Fig. 5.

Kolitsch and Tillmanns (2003) surveyed Pb–(O,OH) clusters. They did not report clusters equivalent to the $[Pb_3(OH)(IO_3)]_2^{8+}$ 'double cluster' (or to the $Pb_3(OH)$ grouping within that cluster) or to the $[Pb_4(OH)_3]^{5+}$ cluster, which are the structural units in the structure of pohlite. However, it is worth noting that both of these clusters have similarities to the well-known cubane-like $[Pb_4(OH)_4]^{4+}$ cluster (Fig. 4d) that occurs in the structures of several minerals: maricopaite (Rouse and Peacor, 1994), bideauxite (Cooper *et al.*, 1999), siidraite (Rumsey *et al.*, 2017), nitroplumbite (Kampf *et al.*, 2022b), cubothioplumbite (Kampf *et al.*, 2022c), hexathioplumbite (Kampf *et al.*, 2022d), hayelasdiite (Kampf *et al.*, 2022e) and finescreekite (Kampf *et al.*, 2022f). Each side of the $[Pb_3(OH)(IO_3)]_2^{8+}$ 'double cluster' is topologically equivalent to the cubane-like $[Pb_4(OH)_4]^{4+}$ cluster with the I^{5+} taking the place of one of the four Pb^{2+} and three O^{2-} taking the place of OH^- groups (Fig. 4b). The $[Pb_4(OH)_3]^{5+}$ cluster is essentially the same as the $[Pb_4(OH)_4]^{4+}$ cluster with one OH^- group removed (Fig. 4c,d).

Seeligerite, $Pb_3^{2+}(I^{5+}O_3)OCl_3$ (Bindi *et al.*, 2008), and schwartzembergite, $Pb_5^{2+}H_2I^{3+}O_6Cl_3$ (Welch *et al.*, 2001) are the only other minerals with compositions similar to that of pohlite; however, these minerals have crystal structures that are very different from one another and from that of pohlite. In addition, schwartzembergite contains I^{3+}, rather than I^{5+}.

Acknowledgements. Reviewers John M. Hughes, Oleg Siidra and Structures Editor Peter Leverett are thanked for their comments on the manuscript. A portion of this study was funded by the John Jago Trelawney Endowment to the Mineral Sciences Department of the Natural History Museum of Los Angeles County.

Supplementary material. To view supplementary material for this article, please visit https://doi.org/10.1180/mgm.2022.123

Competing interests. The authors declare none.

References

Bindi L., Welch M.D., Bonazzi P., Pratesi G. and Menchetti S. (2008) The crystal structure of seeligerite, $Pb_3IO_4Cl_3$, a rare Pb–I-oxychloride from the San Rafael mine, Sierra Gorda, Chile. *Mineralogical Magazine*, **72**, 771–783.

Boric R., Diaz F. and Maksaev V. (1990) Geologia y yacimientos metaliferos de la region de Antofagasta. *Servicio Nacional de Geologia y Mineria Boletin*, **40**, 246 pp.

Brese N.E. and O'Keeffe M. (1991) Bond-valence parameters for solids. *Acta Crystallographica*, **B47**, 192–197.

Cooper M.A., Hawthorne F.C., Merlino S., Pasero M. and Perchiazzi N. (1999) Stereoactive lone-pair behavior of Pb in the crystal structure of bideauxite; $Pb_2^{2+}Ag^+Cl_3F(OH)$. *The Canadian Mineralogist*, **37**, 915–921.

Ferraris G. and Ivaldi G. (1988) Bond valence *vs.* bond length in O···O hydrogen bonds. *Acta Crystallographica*, **B44**, 341–344.

Gagné O.C. and Hawthorne F.C (2015) Comprehensive derivation of bond-valence parameters for ion pairs involving oxygen. *Acta Crystallographica*, **B71**, 562–578.

Girase K., Sawant D.K., Patil H.M. and Bhavsar D.S. (2013) Thermal, FTIR and Raman spectral analysis of Cu (II)-doped lead iodate crystals. *Journal of Thermal Analysis and Calorimetry*, **111**, 267–271.

Higashi T. (2001) *ABSCOR*. Rigaku Corporation, Tokyo.

Jensen J.O. (2002) Vibrational frequencies and structural determinations of $Pb_4(OH)_4^{4+}$. *Journal of Molecular Structure: THEOCHEM*, **587**, 111–121.

Kampf, A.R., Harlow, G.E. and Ma, C. (2022a) Pohlite, IMA 2022-043. CNMNC Newsletter 69. *Mineralogical Magazine*, **86**, 988–992, https://doi.org/10.1180/mgm.2022.115.

Kampf A.R., Hughes J.M., Nash B.P. and Marty J. (2022b) Nitroplumbite, $[Pb_4(OH)_4](NO_3)_4$, a new mineral cubane-like $[Pb_4(OH)_4]^{4+}$ clusters from the Burro mine, San Miguel County, Colorado, USA. *The Canadian Mineralogist*, **60**, 787–795.

Kampf A.R., Smith J.B., Hughes J.M., Ma C. and Emproto C. (2022c) Cubothioplumbite, IMA 2021-091. CNMNC Newsletter 65. *Mineralogical Magazine*, **86**, 354–358, https://doi.org/10.1180/mgm.2022.14

Kampf A.R., Smith J.B., Hughes J.M., Ma C. and Emproto C. (2022d) Hexathioplumbite, IMA 2021-092. CNMNC Newsletter 65; *Mineralogical Magazine*, **86**, 354–358, https://doi.org/10.1180/mgm.2022.14

Kampf A.R., Smith J.B., Hughes J.M., Ma C. and Emproto C. (2022e) Hayelasdiite, IMA 2022-021. CNMNC Newsletter 68. *Mineralogical Magazine*, **86**, 854–859, https://doi.org/10.1180/mgm.2022.93.

Kampf A.R., Smith J.B., Hughes J.M., Ma C. and Emproto C. (2022f) Finescreekite, IMA 2022-030. CNMNC Newsletter 68. *Mineralogical Magazine*, **86**, 854–859, https://doi.org/10.1180/mgm.2022.93

Kolitsch U. and Tillmanns E. (2003) The crystal structure of anthropogenic $Pb_2(OH)_3(NO_3)$, and a review of Pb-(O,OH) clusters and lead nitrates. *Mineralogical Magazine*, **67**, 79–93.

Malcherek T. and Schlüter J. (2006) $Cu_3MgCl_2(OH)_6$ and the bond-valence parameters of the OH–Cl bond. *Acta Crystallographica*, **B63**, 157–160.

Mandarino J.A. (2007) The Gladstone–Dale compatibility of minerals and its use in selecting mineral species for further study. *The Canadian Mineralogist*, **45**, 1307–1324.

Pohl D.C. (1986) Supergene gold transport in bromide groundwater (abstract). *Geological Society of America, Abstracts with Programs*, pp. 720.

Rouse R.C. and Peacor D.R. (1994) Maricopaite, an unusual lead calcium zeolite with an interrupted mordenite-like framework and intrachannel Pb_4 tetrahedral clusters. *American Mineralogist*, **79**, 175–184.

Rumsey M.S., Welch M.D., Kleppe A.K. and Spratt J. (2017) Siidraite, $Pb_2Cu(OH)_2I_3$, from Broken Hill, New South Wales, Australia: the third halocuprate(I) mineral. *European Journal of Mineralogy*, **29**, 1027–1030.

Schellenschläger V., Pracht G. and Lutz H.D. (2001) Single-crystal Raman studies on nickel iodate dihydrate, $Ni(IO_3)_2{\cdot}2H_2O$. *Journal of Raman Spectroscopy*, **32**, 373–382.

Sheldrick G.M. (2015a) *SHELXT* – Integrated space-group and crystal-structure determination. *Acta Crystallographica*, **A71**, 3–8.

Sheldrick G.M. (2015b) Crystal structure refinement with *SHELX*. *Acta Crystallographica*, **C71**, 3–8.

Welch M.D., Hawthorne F.C., Cooper M.A. and Kyser T.K. (2001) Trivalent iodine in the crystal structure of schwartzembergite, $Pb_5^{2+}I^{3+}O_6H_2Cl_3$. *The Canadian Mineralogist*, **39**, 785–795.

Welch M.D., Rumsey M.S. and Kleppe A.K. (2016) A naturally-occurring new lead-based halocuprate(I). *Journal of Solid State Chemistry*, **238**, 9–14.

Williams W.C. (1992) *Magmatic and Structural Controls on Mineralization in the Paleocene Magmatic Arc Between 22°40′ And 23°45′ South Latitude, Antofagasta, II Region, Chile*. Ph.D. Dissertation, University of Arizona, USA.

https://doi.org/10.1180/mgm.2022.123 Published online by Cambridge University Press